# Experimental Localization of Kv1 Family Voltage-Gated K$^+$ Channel $\alpha$ and $\beta$ Subunits in Rat Hippocampal Formation

**Michael M. Monaghan,[1] James S. Trimmer,[2] and Kenneth J. Rhodes[1]**

[1]*Neuroscience, Wyeth-Ayerst Research, Princeton, New Jersey 08543, and* [2]*Department of Biochemistry and Cell Biology and Institute for Cell and Developmental Biology, State University of New York, Stony Brook, New York 11794*

In the mammalian hippocampal formation, dendrotoxin-sensitive voltage-gated K$^+$ (Kv) channels modulate action potential propagation and neurotransmitter release. To explore the neuroanatomical basis for this modulation, we used *in situ* hybridization, coimmunoprecipitation, and immunohistochemistry to determine the subcellular localization of the Kv channel subunits Kv1.1, Kv1.2, Kv1.4, and Kv$\beta$2 within the adult rat hippocampus. Although mRNAs encoding all four of these Kv channel subunits are expressed in the cells of origin of each major hippocampal afferent and intrinsic pathway, immunohistochemical staining suggests that the encoded subunits are associated with the axons and terminal fields of these cells. Using an excitotoxin lesion strategy, we explored the subcellular localization of these subunits in detail. We found that ibotenic acid lesions of the entorhinal cortex eliminated Kv1.1 and Kv1.4 immunoreactivity and dramatically reduced Kv1.2 and Kv$\beta$2 immunoreactivity in the middle third of the dentate molecular layer, indicating that these subunits are located on axons and terminals of entorhinal afferents. Similarly, ibotenic acid lesions of the dentate gyrus eliminated Kv1.1 and Kv1.4 immunoreactivity in the stratum lucidum of CA3, indicating that these subunits are located on mossy fiber axons. Kainic acid lesions of CA3 dramatically reduced Kv1.1 immunoreactivity in the stratum radiatum of CA1–CA3, indicating that Kv1.1 immunoreactivity in these subfields is associated with the axons and terminals of the Schaffer collaterals. Together with the results of coimmunoprecipitation analyses, these data suggest that action potential propagation and glutamate release at excitatory hippocampal synapses are directly modulated by Kv1 channel complexes predominantly localized on axons and nerve terminals.

*Key words: long-term potentiation; synaptic plasticity; A-current; dendrotoxin; ibotenic acid; perforant path; mossy fiber; Schaffer collateral;* Shaker

Voltage-gated K$^+$ (Kv) channels play a major role in regulating the excitability of mammalian hippocampal neurons. In these neurons, Kv channels control postsynaptic responses to excitatory input (for review, see Johnston et al., 2000), modulate the amplitude of back-propagating action potentials (Hoffman et al., 1997), control neuronal spike properties and firing frequency (Zhang and McBain, 1995; Golding et al., 1999), and modulate neurotransmitter release (Hu et al., 1991; Dorandeau et al., 1997; Schechter, 1997; Southan and Owen, 1997). In mammals, Kv channels have been divided into four subfamilies, Kv1–Kv4 (Chandy and Gutman, 1995), which differ in their primary structure, biophysical properties, and subcellular localization. The mammalian *Shaker*, or Kv1, subfamily consists of seven members, of which at least five (Kv1.1–Kv1.4 and Kv1.6) are expressed in the hippocampus proper (Sheng et al., 1994; Wang et al., 1994; Veh et al., 1995; Rhodes et al., 1997). Studies using dendrotoxin (DTX) isoforms as selective blockers of Kv1 $\alpha$ subunits have suggested that Kv1 channel complexes are located predominantly on the terminals of intrinsic hippocampal circuits and subcortical afferent inputs, where they directly modulate neurotransmitter release (Dorandeau et al., 1997; Schechter, 1997; Southan and

Owen, 1997; Geiger and Jonas, 2000). Interestingly, studies examining the effects of DTX isoforms with distinct subunit specificity indicate that the responses of hippocampal neurons to Kv1 channel block vary across subfields (Southan and Owen, 1997), suggesting that the subunit composition of Kv1 channel complexes that underlie these responses also vary.

Kv1 channels are complex membrane protein oligomers consisting of four integral membrane pore-forming $\alpha$ subunits and four cytoplasmic $\beta$ subunits. It is now well established that Kv1 $\alpha$ and $\beta$ subunits differentially coassemble, giving rise to $\alpha_4\beta_4$ channel complexes with considerable electrophysiological and biochemical heterogeneity (Sheng et al., 1993; Wang et al., 1993; Scott et al., 1994; Rhodes et al., 1995, 1996, 1997). Although immunohistochemical staining for individual Kv1 subunits in the hippocampus suggests that they are located predominantly on axons and in terminal fields (Sheng et al., 1993, 1994; Wang et al., 1994; Rhodes et al., 1995, 1996, 1997), there are also reports of somatodendritic localization (Sheng et al., 1994; Veh et al., 1995; Rhodes et al., 1996, 1997; Cooper et al., 1998). In the few cases in which ultrastructural studies have been performed (Wang et al., 1994; Cooper et al., 1998), there is clear evidence for localization of Kv1 $\alpha$ subunits along axons and at or near axon terminals but no evidence for localization of these channels to somatodendritic domains.

Although the exquisite laminar segregation of the major hippocampal circuits tempts conclusions regarding protein localization in this structure, it can be difficult to associate staining patterns with specific pathways unless there are clear morphological criteria to establish a the identity of a pathway (e.g., for the

mossy fiber pathway; Acsády et al., 1998). Even multiple-label anatomical techniques cannot reveal the coassociation of individual channel subunits in heteromeric channel complexes. To circumvent these issues, we used a strategy that used circumscribed lesions, immunohistochemistry, and coimmunoprecipitation to determine the association of Kv1.1, Kv1.2, Kv1.4, and Kv$\beta$2 with each of the major afferent, intrinsic, and efferent pathways of the rat hippocampus. Our data suggest that the majority of Kv1 channels present in this structure are heteromeric and associated with the axons and terminals of cortical afferent and intrinsic excitatory projections. Moreover, we find that the subunit composition of Kv1 channel complexes varies across subfields. Our results resolve some of the controversy surrounding Kv1 subunit localization in hippocampal formation and underscore the importance of Kv1 channels in regulating axonal excitability and neurotransmitter release in circuits that play a key role in memory processes and synaptic plasticity.

## MATERIALS AND METHODS

*Materials.* All reagents were molecular biology grade from Sigma (St. Louis, MO) or Roche Molecular Biochemicals (Indianapolis, IN), except where noted otherwise.

In situ *hybridization histochemistry.* DNA templates for riboprobe synthesis were prepared by PCR from the full-length cDNA clones of the corresponding subunits (Nakahira et al., 1996). All riboprobe sequences were compared by BLAST to the GenBank database to verify that they will only recognize the appropriate targets among all deposited sequences. The riboprobe used to localize Kv$\beta$2 mRNA was described previously (Rhodes et al., 1996). A riboprobe for the Kv1.1 subunit was generated using a pair of oligonucleotide primers designed to amplify a 335 bp region spanning nucleotides 1735–2070 of the rat Kv1.1 cDNA and, in addition, add the promoter sequences for T7 (forward) and T3 (reverse) polymerase. These primers contained the following sequences: 5′-TAATACGACTCACTAT-AGGGAAAAAAGCACCAGGCAAGCA-3′ (forward) and 5′-ATTA-ACCCTCACTAAAGGGAACACAGACTA CTTCATGGGC-3′ (reverse). A riboprobe for the Kv1.2 subunit was generated using a pair of primers designed to amplify a 443 bp region spanning nucleotides 1111–1544 of the rat Kv1.2 cDNA and, in addition, add the promoter sequence for T3 polymerase. These primers had the following sequences: 5′-GCTGATGAGCGAGATTCCCAGTTCC-3′ (forward) and 5′-AATTA-ACCCTCACTAAAGGGATCAGTTAACATTTT-GGTAA-3′ (reverse). A riboprobe for the Kv1.4 subunit was generated using a pair of primers designed to amplify a 496 bp region spanning nucleotides 70–566 of the rat Kv1.4 cDNA and, in addition, add the promoter sequence for T3 polymerase. These primers had the following sequences: 5′-AAACTAC-CACCATGGAGGTGGCAAT-3′ (forward) and 5′-AATTAACCCT-CACTAAAGGGGCTCTGCCTGTGGTGGAGTT-3′ (reverse). All PCR products were gel-purified on 1.5% low-melt agarose gels. Bands containing the PCR products were excised, phenol- and then phenol-chloroform-extracted, and ethanol-precipitated. The pellet was then dried and resuspended in 1× TE buffer (10 mM Tris-HCl and 1 mM EDTA, pH 7.4). Fifty nanograms of DNA template was used for *in vitro* transcription reactions using [$^{35}$S]CTP (New England Nuclear, Boston, MA) and the Riboprobe Gemini System (Promega, Madison, WI). Each of these riboprobes was used for *in situ* hybridization histochemistry as described previously (Rhodes et al., 1996). After the hybridization reaction, sections were apposed to Hyperfilm (Amersham Pharmacia Biotech, Arlington Heights, IL) for 3–10 d and subsequently dipped in nuclear track emulsion (NTB-2; Eastman Kodak, Rochester, NY) to obtain higher-resolution autoradiograms.

To assess nonspecific labeling in the *in situ* hybridization procedure, a control probe was generated from a template provided in the Riboprobe Gemini System kit (Promega catalog #P2651). This vector was linearized using *Sca*I and transcribed using T3 polymerase. The resulting transcription reaction generated two riboprobes, one a 250 bp product and the other a 1525 bp product, comprising only vector sequence. This control probe mixture was labeled as described above and added to the hybridization solution at a final concentration of 50,000 cpm/$\mu$l. No specific hybridization was observed in control sections; i.e., these sections gave a weak, uniform hybridization signal (results not shown).

*Immunoprecipitation.* Immunoprecipitation reactions (Rhodes et al.,

1995, 1996, 1997) were performed at 4°C using detergent lysates of a crude membrane fraction (Trimmer, 1991) isolated from freshly dissected adult rat hippocampi. In brief, hippocampal membranes (1 mg of membrane protein per tube) were solubilized in lysis buffer (1% Triton X-100, 0.15 M NaCl, 1 mM EDTA, 10 mM sodium azide, 10 mM and Tris-HCl, pH 8.0) containing a protease inhibitor mixture. Affinity-purified antibodies specific for each subunit (Rhodes et al., 1995, 1996) were added, and the volume was adjusted with lysis buffer to 1 ml/reaction tube. Samples were incubated for 2 hr on a rotator, followed by addition of 50 $\mu$l of a 50% slurry of protein A-agarose and further incubation for 45 min. After incubation, protein A-Sepharose was centrifuged at 10,000 × g for 20 sec, and the resulting pellets were washed by resuspension and centrifugation six times with lysis buffer. The final pellets were resuspended in 240 $\mu$l of reducing sample buffer.

*SDS-polyacrylamide gels and immunoblotting.* Samples were size-fractionated on 9% (for analysis of $\alpha$ subunits) or 12% (for analysis of $\beta$ subunits) SDS-PAGE. Crude synaptosomal membrane fractions from whole brain [rat brain membrane("RBM"); 30 $\mu$g] or from rat hippocampus [rat hippocampal membranes ("RHCM"); 20 $\mu$g] were added to SDS sample buffer, boiled, and loaded directly. For immunoprecipitation reactions, 20 $\mu$l of sample, representing the reaction product from 83 $\mu$g of hippocampal membranes, was loaded. Disulfide bonds were reduced by the addition of 20 mM 2-mercaptoethanol to the sample buffer. Lauryl sulfate (Sigma) was the SDS source used for all SDS-PAGE (Shi et al., 1994). After electrophoretic transfer to nitrocellulose paper, the resulting blots were blocked in Tris-buffered saline (TBS) containing 4% low-fat milk (Blotto; Johnson et al., 1984), incubated in affinity-purified antibody diluted 1:50–1:2000 in Blotto for 1 hr or undiluted mAb tissue culture supernatant (K17/70 anti-Kv$\beta$2), and washed three times in Blotto for 30 min total. Blots were then incubated in HRP-conjugated secondary antibody (Cappel, West Chester, PA; 1:2000 dilution in Blotto) for 1 hr and then washed in TBS three times for 30 min total. The blots were then incubated in substrate for enhanced chemiluminescence (ECL) for 1 min and autoradiographed on preflashed (to OD$_{545}$ = 0.15) Fuji (Tokyo, Japan) RX or Kodak XAR-5 film.

*Experimental localization of channel subunits.* All surgical procedures were approved by the Wyeth-Ayerst Institutional Animal Care and Use Committee and were in accordance with the National Institutes of Health *Guide for the Care and Use of Laboratory Animals.* Before surgery, animals were deeply anesthetized with sodium pentobarbital (50 mg/kg, i.p.) and secured in a stereotaxic carrier (David Kopf Instruments, Tajunga, CA). For lesions of the dentate gyrus, hippocampal subfields, or the entorhinal cortex, ibotenic acid (0.1–0.4 $\mu$l of a 10 $\mu$g/$\mu$l solution in 0.1 M sodium phosphate buffer, pH 7.4) was injected directly into the target structure using a 2 $\mu$l Hamilton (Reno, NV) microsyringe mounted in a Kopf microsyringe microdrive. In some of these animals, injections were made at two or three depths, with each injection separated in the dorsoventral axis by 2.5 mm. To generate lesions encompassing the entire CA3 subfield, kainic acid (1 $\mu$l of a 1 $\mu$g/$\mu$l solution in 0.1 M NaPO$_4$ buffer) was injected into the lateral cerebral ventricle immediately adjacent to CA3 (procedure modified from that of Bernard and Wheal, 1995). To examine the association of individual subunits with subcortical afferents, transections of the fornix were made unilaterally using a specially constructed Scouten wire knife (Kopf). To produce the lesion, the guide cannula of the knife was lowered under stereotaxic control to a point just beneath the fornix. The wire knife was then extended 2 mm medially in the coronal stereotaxic plane, raised 4.5 mm, and then retracted. The knife was then again lowered, and the wire was extended 2 mm laterally in the coronal stereotaxic plane and then raised 4.5 mm to complete the transection. To verify that the fornix transections were complete, one series of sections from each case was processed using acetylcholinesterase (AChE) histochemistry, as described previously (Tago et al., 1986).

*Immunohistochemistry.* After a 7 d postsurgical survival, all animals were deeply anesthetized with sodium pentobarbital (60 mg/kg, i.p.) and then perfused through the ascending aorta with 0.1 M NaPO$_4$ buffer, pH 7.4, followed by fixative containing freshly depolymerized 4% paraformaldehyde in 0.1 M NaPO$_4$ buffer. The remaining procedures for light microscopic immunohistochemistry using these same subunit-specific affinity-purified rabbit polyclonal antibodies have been described in detail previously (Rhodes et al., 1995, 1996). Briefly, 40-$\mu$m-thick horizontal sections were incubated overnight at 4°C in antibody vehicle containing affinity-purified rabbit polyclonal antibodies. Detection of antibody–antigen complexes was accomplished using the ABC Elite peroxidase reaction (Vector Laboratories, Burlingame, CA) and visual-
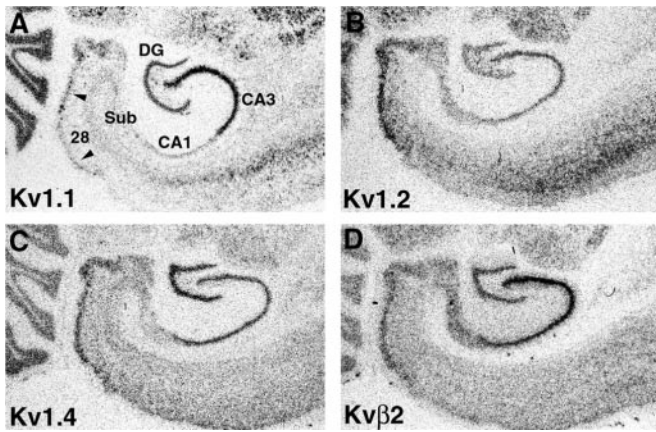
*Figure 1.* Expression of Kv1 $\alpha$ and $\beta$ subunit mRNAs in the rat temporal lobe. These photographs of film autoradiograms show the pattern of expression of Kv1.1, Kv1.2, Kv1.4, and Kv$\beta$2 mRNA in the rat entorhinal cortex (area 28) and hippocampal formation. Areas with high levels of mRNA expression appear as *darker regions* in these bright-field images. There is a high level of mRNA expression for these four subunits in layer II of the entorhinal cortex (*arrowheads*) and in the principal cells of all hippocampal subfields (CA1–CA4). In contrast to the fairly uniform expression of Kv1.2, Kv1.4, and Kv$\beta$2 mRNA across hippocampal subfields, there is a much greater density of Kv1.1 mRNA expression in the stratum pyramidale of CA3 in comparison with the other subfields. *28*, Entorhinal cortex; *DG*, dentate gyrus; *Sub*, subiculum.

ized using a nickel-enhanced diaminobenzidine procedure (Tago et al., 1986; Rhodes et al., 1995).

Stained sections and autoradiograms generated by *in situ* hybridization were analyzed and photographed using a Zeiss (Thornwood, NY) Axiophot photomicroscope. Low-magnification photographs of these specimens were taken using a Nikon (Melville, NY) Multiphot macrophotography system. Black-and-white 35 mm film negatives were digitally imaged using a Nikon LS1000 35 mm film scanner. The scanned images were arranged and labeled in Adobe (Mountain View, CA) Photoshop with only minor adjustments of image brightness and contrast.

## RESULTS

### Localization of Kv $\alpha$ and $\beta$ subunit mRNA in the rat hippocampus

Analysis of Kv1.1, Kv1.2, Kv1.4, and Kv$\beta$2 expression by *in situ* hybridization revealed that mRNAs encoding these subunits are expressed in neurons that give rise to the major cortical afferent input and the major intrinsic projections of the rat hippocampal formation. For example, mRNAs encoding Kv1.1, Kv1.2, Kv1.4, and Kv$\beta$2 are highly expressed in the large multipolar neurons in layer II of the entorhinal cortex that give rise to the perforant pathway, and moderate to high levels of these four subunit mRNAs are expressed in the granule and infragranular neurons in the dentate gyrus (Fig. 1). Similarly, there are moderate to high levels of expression of all four subunit mRNAs in the stratum pyramidale of the CA subfields, prosubiculum, and subiculum. The expression level of Kv1.1 mRNA in the CA subfields is not uniform: there is a far greater density of Kv1.1 expression in the stratum pyramidale of CA3 compared with CA1 or the subiculum (Séquier et al., 1990; Wang et al., 1994). Analysis of emulsion autoradiograms (results not shown) indicated that in addition to their expression in CA1–CA3 pyramidal cells, Kv1.1, Kv1.2, Kv1.4, and Kv$\beta$2 mRNAs are also expressed in some small to medium-sized interneurons in the stratum oriens and stratum radiatum of the CA subfields.
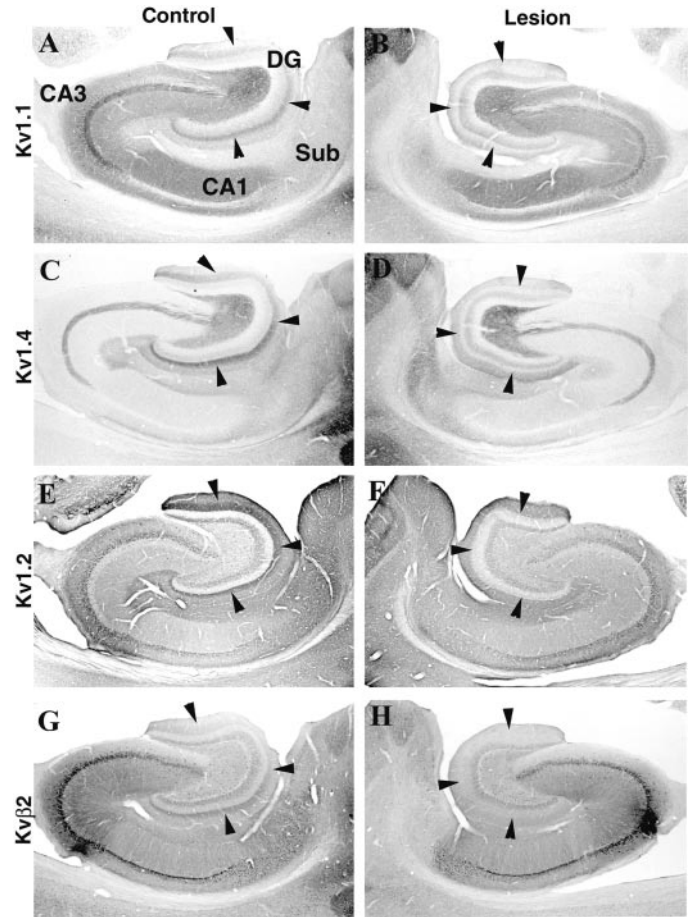


*Figure 2.* Effects of an ibotenic acid lesion in the entorhinal cortex on Kv1 $\alpha$ and $\beta$ subunit immunoreactivity in the hippocampus. These photomicrographs show the pattern of immunoreactivity for Kv1.1, Kv1.4, Kv1.2, and Kv$\beta$2 in the hippocampus of the unoperated control hemisphere (*A, C, E, G*) and in the operated hemisphere (*B, D, F, H*) of an animal that sustained a large unilateral ibotenic acid lesion in the entorhinal cortex. In the control hemisphere, there is a distinct band of immunoreactivity for all four subunits in the middle third of the molecular layer of the dentate gyrus (*arrowheads*). The location of this band corresponds to the termination zone of projections from the medial entorhinal cortex to the dentate gyrus. After the ibotenic acid lesion, the band of immunoreactivity for Kv1.1 and Kv1.4 in the ipsilateral dentate gyrus is eliminated (*B, D, arrowheads*), and the band of immunoreactivity for Kv1.2 and Kv$\beta$2 is greatly diminished in intensity (*F, H, arrowheads*). *DG*, Dentate gyrus; *Sub*, subiculum.

### Immunoreactivity for Kv1.1, Kv1.2, Kv1.4, and Kv$\beta$2 in the rat hippocampus

The general pattern of immunoreactivity for the Kv1.1, Kv1.2, Kv1.4, and Kv$\beta$2 polypeptides in the rat hippocampus has been described previously (Sheng et al., 1993; Wang et al., 1993, 1994; Rhodes et al., 1995, 1996, 1997; Veh et al., 1995; Cooper et al., 1998). To briefly summarize, immunoreactivity for each of these subunits appears to be concentrated in the axons and at or near the axon terminals of cells expressing the corresponding mRNAs, with a much lower density of staining associated with the somatodendritic membranes of hippocampal neurons (Fig. 2*B–E*) (Sheng et al., 1993; Wang et al., 1994; Rhodes et al., 1997; Cooper et al., 1998). The exception to this pattern is Kv$\beta$2. In addition to staining of axons and terminal fields, Kv$\beta$2 appears to be concentrated in the somata and throughout the apical dendrites of

dentate granule cells and hippocampal pyramidal cells (Rhodes et al., 1997).

Although we can reasonably infer the subcellular distribution and pathway association of individual subunits on the basis of a comparison of mRNA expression and immunohistochemical staining patterns, it is not possible to associate staining for individual subunits with specific pathways using this type of data alone. For example, in the dentate gyrus, there is a dense band of immunoreactivity for Kv1.1, Kv1.2, Kv1.4, and Kvβ2 in the middle third of the molecular layer (Fig. 2). The location of this band corresponds closely to the pattern of termination of afferents from the medial entorhinal cortex (Steward, 1976; Steward and Scoville, 1976; Wyss, 1981; Rhodes et al., 1997; Dolorfo and Amaral, 1998). Given the high levels of mRNA expression for these four Kv1 subunits in layer II of the entorhinal cortex, one reasonable interpretation of the immunohistochemical data is that the band of immunoreactivity in the dentate molecular layer reflects localization of these subunits to the axons and terminals of the medial perforant path. Similarly, in the stratum radiatum and stratum oriens of CA1–CA3, there is a wide zone of immunoreactivity for Kv1.1. This zone of immunoreactivity for Kv1.1 is confined to the stratum radiatum and stratum oriens and closely matches the termination zones of the associational and commissural components of the Schaffer collateral pathway (Swanson et al., 1978; Ishizuka et al., 1990). Given the very high expression of Kv1.1 mRNA in CA3 pyramidal cells, one reasonable interpretation of the immunohistochemical data is that Kv1.1 is localized to the axons and terminals of the Schaffer collateral projection. However, an equally reasonable interpretation of the immunohistochemical data, in both the dentate gyrus and CA1 subfields, is that these subunits are targeted and localized to a defined region of granule or pyramidal cell dendrites. In the absence of other data, it is difficult to determine which interpretation is correct. Another level of complexity inherent in the immunohistochemical data is that although individual subunits appear to be colocalized, the relative abundance of individual subunits in each pathway, and the corresponding subunit composition of the channel complexes, may be distinct. Even where the staining patterns for individual subunits overlap, we cannot conclude that the subunits are associated with the same pathway or even localized to the same subcellular domain. To address these issues and to more precisely associate the staining patterns with specific hippocampal circuits, we destroyed the cells of origin of each circuit with an axon-sparing neurotoxin, ibotenic acid (Kohler and Schwarcz 1983; Erselius and Wree, 1991), and then examined in sequential sections the effects on the staining pattern for all four subunits.

## Experimental analysis of Kv subunit expression using ibotenic acid lesions

### Ibotenic acid lesions of the entorhinal cortex
Large unilateral ibotenic acid lesions of the entorhinal cortex were made in eight animals. In each animal, four separate injections of ibotenic acid were made into the right entorhinal cortex, with each injection spaced 2.5 mm apart in the dorsoventral axis. Although these lesions destroyed almost the entire entorhinal cortex, analysis of sections stained for Nissl substance revealed that the most ventral and lateral entorhinal areas and the entire dentate gyrus were spared in all cases.

An example of the effects of one of these large entorhinal ibotenic acid lesions is shown in Figure 2. This lesion resulted in virtually complete destruction of cells in the entorhinal cortex

and, in concert with the degeneration of the axons and terminals of entorhinal afferents, led to profound gliosis within the middle third of the molecular layer of the dentate gyrus and in the stratum moleculare of CA1–CA3 (results not shown). When compared with the nonoperated control hemisphere (Fig. 2A), it is clear that this lesion produced a dramatic effect on Kv1.1, Kv1.2, Kv1.4, and Kvβ2 immunoreactivity in the dentate gyrus (Fig. 2A–H). For example, the dense band of Kv1.1 and Kv1.4 immunoreactivity in the middle third of the dentate molecular layer was eliminated (Figs. 2A–D, 3A,B), and there appeared to be a shift in the staining pattern for Kv1.2 and Kvβ2 such that the bands of Kv1.2 and Kvβ2 immunoreactivity became more diffuse and occupied the outer half of the molecular layer instead of being concentrated in the middle third (Figs. 2E–H, 3C,D). Interestingly, in the ipsilateral dentate gyrus there was an increase in the overall intensity of Kv1.1, Kv1.2, and Kv1.4 immunoreactivity (see below). This entorhinal cortex lesion also reduced the density of Kv1.1, Kv1.2, Kv1.4, and Kvβ2 immunoreactivity in the stratum moleculare of CA1–CA3. This loss of immunoreactivity was caused by the loss of axons and terminals of entorhinal layer II and III neurons that form the ammonic component of the perforant path (Steward and Scoville, 1976; Witter et al., 1988).

The changes observed after ibotenic acid lesions of the entorhinal cortex suggest that in the dentate gyrus, all four subunits are located on the axons and at or near the terminals of entorhinal afferents. These results are consistent with the electron microscopic observations of Wang et al. (1994) and Cooper et al. (1998), who demonstrated that in the dentate gyrus, Kv1.1 Kv1.2, and Kv1.4 immunoreactivity is contained within axons and axon terminals in the middle third of the molecular layer. Our results also indicate that, on the side of the lesion, there is a compensatory increase in the density of Kv1.1, Kv1.2, Kv1.4, and Kvβ2 immunoreactivity in the inner and outer thirds of the dentate molecular layer. However, it is not clear from these data whether these changes in immunoreactivity are attributable to the degeneration of presynaptic axons and terminals from the entorhinal cortex or to postsynaptic changes in granule cell dendrites (i.e., loss or reorganization of synapses) evoked by loss of entorhinal input, or both. To distinguish between these possibilities, we made ibotenic acid lesions in the dentate gyrus and examined the effects of this complementary lesion on the distribution and density of Kv1 subunit immunoreactivity.

### Ibotenic acid lesions of the dentate gyrus
Seven animals sustained a unilateral lesion of the dentate gyrus. In each animal, a single injection of ibotenic acid was made at approximately the midpoint of the dorsoventral axis of the hippocampus. In most animals the lesion destroyed neurons within a small sphere of tissue that included the dentate gyrus and spread across the hippocampal fissure into the distal CA1 subfield and subiculum (Fig. 4). For these dentate gyrus lesions, we restricted our analyses to animals from which analysis of sections stained for Nissl substance revealed that there was little or no spread of the toxin into the CA3 subfield. This lesion destroyed dentate granule cells and hilar neurons and, in addition, killed neurons in the distal CA1 subfield and the subiculum. There was also some shrinkage of the dentate gyrus itself (Fig. 4, compare A, B), presumably because of loss of dentate granule cells and their dendritic volume.

Despite the loss of dentate granule cells, the distribution of immunoreactivity for Kv1.1, Kv1.2, Kv1.4, and Kvβ2 in the dentate molecular layer was not affected by this lesion (Fig. 4C–J).
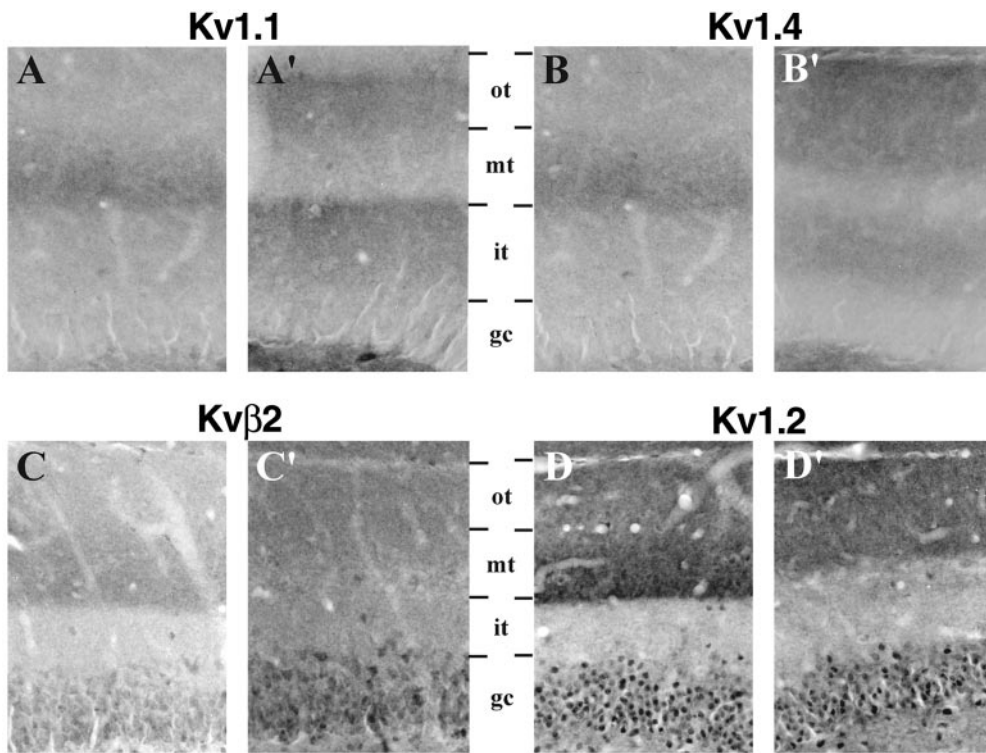
*Figure 3.* Effects of an ibotenic acid lesion in the entorhinal cortex on Kv1 $\alpha$ and $\beta$ subunit immunoreactivity in the dentate gyrus. These high-magnification photomicrographs were taken from the same animal shown in Figure 2 and demonstrate the pattern of immunoreactivity for Kv1.1, Kv1.4, Kv$\beta$2, and Kv1.2 in the dentate gyrus of the unoperated control hemisphere (*A–D*) and in the hemisphere that sustained a large ibotenic acid lesion in the entorhinal cortex (*A'– D'*). Each pair of photomicrographs is aligned on the dentate granule cell layer (*gc*) to facilitate comparison of the staining patterns in the two hemispheres. After the entorhinal cortex lesion, the distinct band of immunoreactivity for Kv1.1 (*A'*) and Kv1.4 (*B'*) in the middle third (*mt*) of the molecular layer is virtually eliminated in the operated hemisphere. In the inner third (*it*) and outer third (*ot*) of the molecular layer, however, the density of Kv1.1 and Kv1.4 immunoreactivity appears to increase. The effects of the entorhinal cortex lesion on Kv$\beta$2 (*C*) and Kv1.2 (*D*) immunoreactivity were somewhat different from for Kv1.1 and Kv1.4. The density of Kv$\beta$2 and Kv1.2 in the middle third of the molecular layer is clearly diminished, but there remains a band of Kv$\beta$2 and Kv1.2 immunoreactivity in the outer half of the molecular layer.

The normally dense band of Kv1.1, Kv1.2, Kv1.4, and Kv$\beta$2 immunoreactivity in the middle third of the molecular layer remained. Moreover, in the middle third of the molecular layer, there actually appeared to be an increase in the density of reaction product for all four subunits, suggesting that there may have been a compensatory increase in Kv1 subunit expression in response to this lesion. Together with the data described above, these results strongly suggest that in the middle third of the molecular layer of the dentate gyrus, the changes in immunoreactivity observed after entorhinal ibotenic acid lesions were attributable to loss of entorhinal afferents and not loss of postsynaptic targets.

Another pronounced effect of ibotenic acid lesions in the dentate gyrus was that the high density of Kv1.1 and Kv1.4 immunoreactivity in the stratum lucidum of CA3 was completely eliminated (Fig. 4*D,F*). Because dentate granule cells were destroyed by this lesion but CA3 pyramidal cells appeared unaffected, this result indicates that these two subunits are located on the axons of the mossy fiber pathway. This finding is consistent with our previous interpretations of this staining pattern (Rhodes et al., 1995, 1997) and with the results of recent electron microscopic analyses (Cooper et al., 1998). However, it is conceivable that these changes in Kv1.1 and Kv1.4 immunoreactivity in the CA3 subfield resulted from postsynaptic changes in CA3 pyramidal cells resulting from loss of mossy fiber input. To address this issue, we made ibotenic acid lesions of the CA3 subfield and examined the effects on the distribution and density of Kv1 channel subunits.

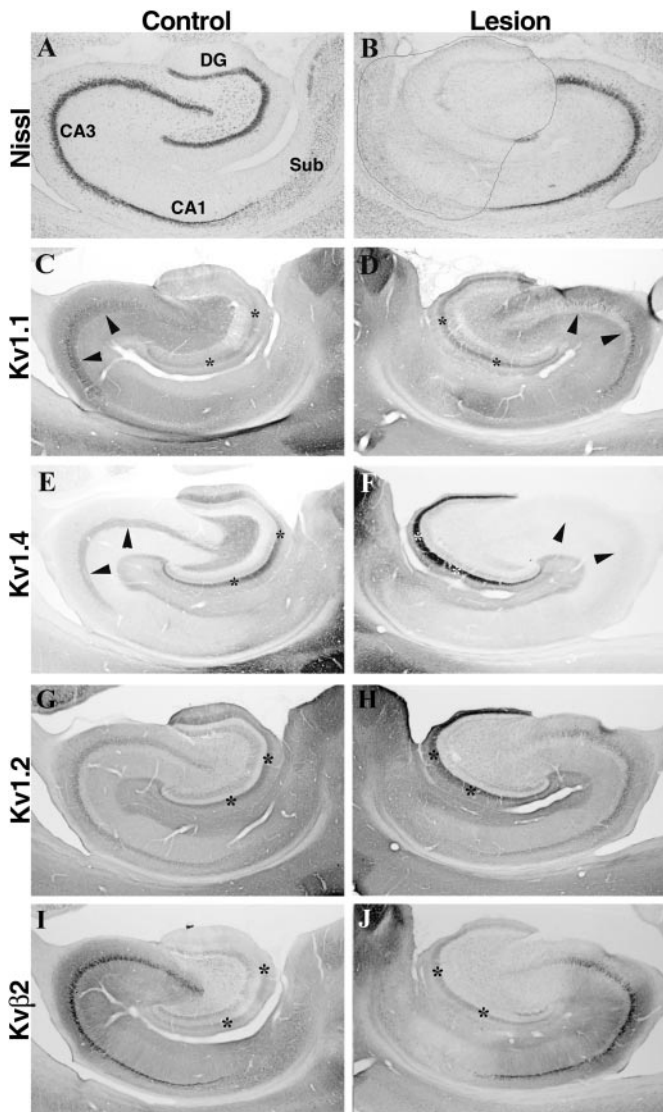*Ibotenic acid lesions of the CA3 subfield*
Nine animals sustained a large unilateral ibotenic acid lesion of the CA3 subfield. In each animal, a single injection of ibotenic acid was made at a middorsoventral level of the hippocampus. In most animals the lesion destroyed a 1–2 mm sphere of tissue that

included the CA3 subfield, a small amount of CA2, and the proximal third of CA1. In other animals, the CA3 lesion was smaller and entirely confined to CA3 (Fig. 5*B*).

Ibotenic acid lesions within the CA3 subfield had little effect on the distribution or density of Kv1.1 and Kv1.4 immunoreactivity in the stratum lucidum (Fig. 5*D,F*), although there was a dramatic loss of CA3 pyramidal cells within the boundaries of the lesion (Fig. 5*B*). This result confirms that the immunoreactivity for Kv1.1 and Kv1.4 in the stratum lucidum is associated with mossy fiber axons, and that the loss of immunoreactivity for Kv1.1 and Kv1.4 observed after ibotenic acid lesions of the dentate gyrus was attributable to destruction of the cells of origin of the mossy fiber pathway (the dentate granule cells) and not to a loss of postsynaptic targets in CA3.

Surprisingly, ibotenic acid lesions in the CA3 subfield produced an increase in the density of Kv1.1 immunoreactivity within the boundaries of the lesion (Fig. 5*D*). Although the reason for this increased staining is unclear, it may be attributable to a compensatory increase in Kv1.1 protein expression in the axons of the Schaffer collaterals originating from cells outside the boundaries of this lesion.

As described above and in our earlier publications (Rhodes et al., 1997), one interpretation of the Kv1.1 staining pattern in the stratum radiatum of CA3 and CA1 is that this subunit is located on the axons and at or near the axon terminals of the Schaffer collateral pathway. This interpretation is consistent with the very high level of Kv1.1 mRNA expression in the CA3 subfield and with electron microscopic analyses demonstrating Kv1.1 immunoreactivity in axons and presynaptic terminals in the stratum radiatum of CA1 but not in the dendrites of CA1 pyramidal cells (Wang et al., 1994). Because of this, we were somewhat surprised to see that ibotenic acid lesions in CA3 did not produce a detectable decrease in Kv1.1 immunoreactivity in the stratum

*Figure 4.* Effects of an ibotenic acid lesion in the dentate gyrus on Kv1.1 and Kv1.4 immunoreactivity in the dentate gyrus and CA3 subfield. Photomicrographs show sections taken from an animal that sustained a unilateral injection of ibotenic acid into the dentate gyrus. As shown in the sections stained for Nissl substance (*A, B*), this ibotenic acid lesion killed virtually all dentate granule cells as well as neurons in CA4, the distal end of CA1, and the subiculum. Neurons in the CA3 subfield were not affected by this lesion. This lesion did not appear to reduce the density of Kv1.1 (compare *C, D*) or Kv1.4 (compare *E, F*) immunoreactivity in the middle third of the dentate molecular layer (*asterisks*). Moreover, this lesion did not alter the density of Kv1.2 (*G, H*) or Kvβ2 (*I, J*) immunoreactivity in the molecular layer of the dentate gyrus. These results are consistent with those shown in Figures 2 and 3 and indicate that the dense band of Kv1.1 and Kv1.4 immunoreactivity in the dentate molecular layer is associated with entorhinal afferents and not the dendrites of dentate granule cells. Interestingly, this dentate gyrus lesion virtually eliminated the band of Kv1.1 and Kv1.4 immunoreactivity in the stratum lucidum of CA3 (*arrowheads*). Because the axons and terminals of dentate granule cells (the mossy fibers) were destroyed by this ibotenic acid lesion, this result indicates that Kv1.1 and Kv1.4 are associated with mossy fiber axons. *DG*, Dentate gyrus; *Sub*, subiculum.

radiatum of CA3 or CA1. One explanation for the lack of an effect is that the axons of CA3 pyramidal cells forming the Schaffer collateral pathway are highly branched and form extensive connections along the septotemporal axis of the hippocampus
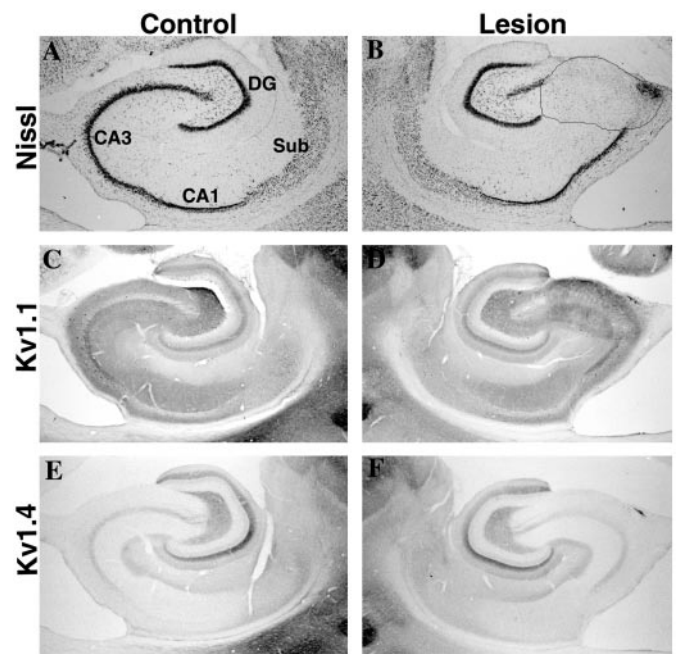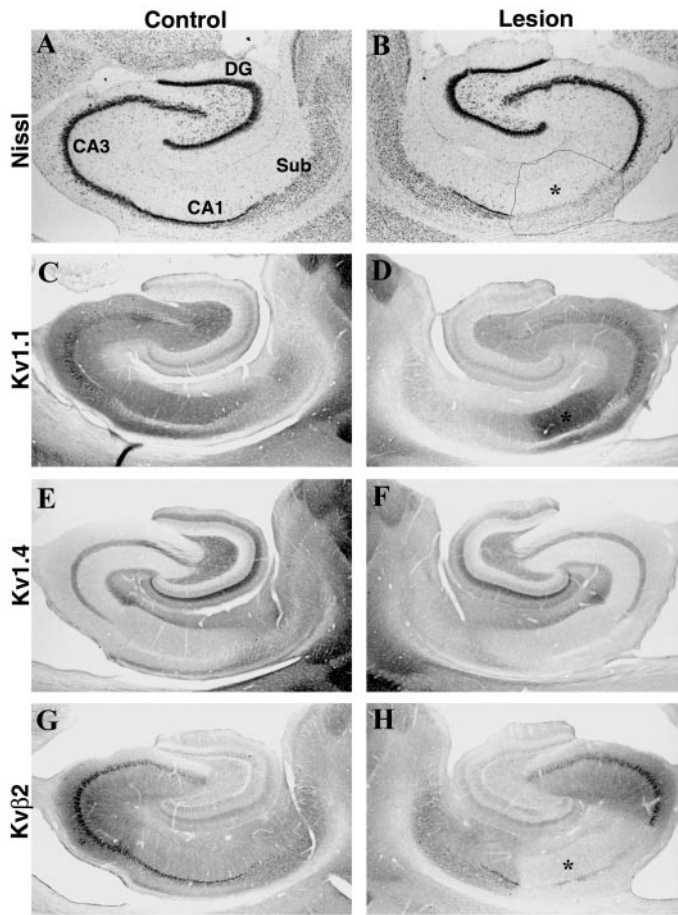


*Figure 5.* Effects of an ibotenic acid lesion in the CA3 subfield on Kv1.1 and Kv1.4 immunoreactivity in the CA3 and CA1 subfields. Photomicrographs show sections taken from an animal that sustained a unilateral injection of ibotenic acid in CA3. As shown in the sections stained for Nissl substance (*A, B*), this ibotenic acid lesion killed neurons in the CA3 subfield only. This lesion did not appear to reduce the density of Kv1.1 (compare *C, D*) or Kv1.4 (compare *E, F*) immunoreactivity in the stratum lucidum of CA3. This result is consistent with the data in Figure 4, which indicated that in stratum lucidum of CA3, Kv1.1 and Kv1.4 immunoreactivity is associated with axons of the mossy fiber pathway and not with the dendrites of CA3 pyramidal cells. As described in Results, this discrete lesion in CA3 did not alter the density of Kv1.1 or Kv1.4 (or Kv1.2 or Kvβ2; results not shown) immunoreactivity in other hippocampal subfields. *DG*, Dentate gyrus; *Sub*, subiculum.

(Tamamaki and Nojyo, 1988; Ishizuka et al., 1990). As a result, our circumscribed ibotenic acid lesions may not have destroyed enough CA3 pyramidal cells to significantly reduce the number of Schaffer collateral axons in CA1 even at levels immediately adjacent to the lesion.

### Ibotenic acid lesions in the CA1 subfield

Unilateral ibotenic acid lesions of the CA1 subfield were made in three animals. In each animal, a single injection of ibotenic acid was made at a middorsoventral level of the hippocampus. In most animals, the ibotenic acid lesion destroyed neurons within a 1–3 mm sphere of tissue and involved virtually all of the CA1 subfield plus some of the adjacent CA2 subfield, prosubiculum, and subiculum. In some cases, these lesions also destroyed a portion of the dentate gyrus. However, analysis of sections stained for Nissl substance revealed that in all of these cases the CA3 subfield was almost entirely spared.

An example of the effects of a CA1 ibotenic acid lesion is shown in Figure 6. In this animal, the lesion destroyed the entire CA2 and the proximal three-fourths of the CA1 subfield but spared all but the most distal tip of CA3 and completely spared the subiculum. This lesion eliminated immunoreactivity for Kvβ2 in the somata and dendrites of CA1 pyramidal cells (Fig. 6*H*). As described above for the ibotenic acid lesion in CA3, the density of Kv1.1 immunoreactivity in the stratum radiatum and stratum oriens increased within the boundaries of the lesion, but the
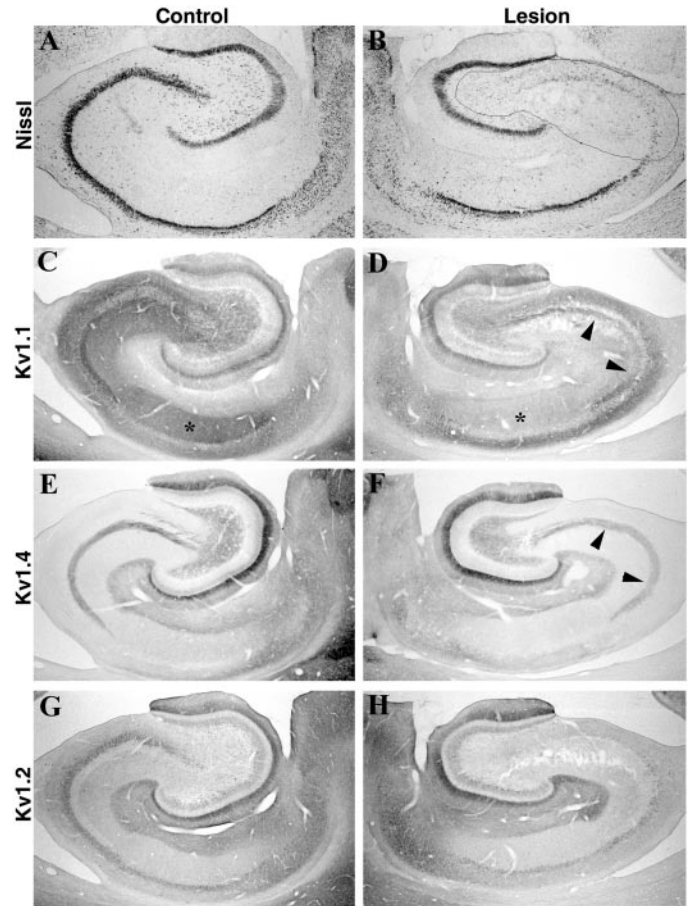
*Figure 6.* Effects of an ibotenic acid lesion in the CA1 subfield on Kv1 $\alpha$ and $\beta$ subunit immunoreactivity in CA1. Photomicrographs show sections taken from an animal that sustained a unilateral injection of ibotenic acid in CA1. As shown in the sections stained for Nissl substance (*A, B*), this ibotenic acid lesion killed neurons in CA1, CA2, and the distal tip of CA3. This lesion produced a slight increase in the density of Kv1.1 immunoreactivity within the boundaries of the lesion (*D, asterisk*) but did not affect the density of Kv1.4 (*E, F*). This result is consistent with our interpretation that the majority of Kv1.1 (and Kv1.4) immunoreactivity in CA1 is associated with the axons and terminals of the Schaffer collateral pathway and not with the apical dendrites of CA pyramidal cells. This CA1 lesion also dramatically reduced the density of Kv$\beta$2 immunoreactivity within the boundaries of the lesion (*H, asterisk*). This result is consistent with our previous interpretations (Rhodes et al., 1996, 1997) that Kv$\beta$2 is concentrated in the somata and apical dendrites of hippocampal pyramidal cells. *DG*, Dentate gyrus; *Sub*, subiculum.

density of Kv1.2 (results not shown) and Kv1.4 (Fig. 6*F*) immunoreactivity was unchanged. Similarly, within the boundaries of the lesion, the density of Kv1.2 and Kv1.4 immunoreactivity in the stratum moleculare of CA1 was unchanged. Together with the results of the other lesions, these data suggest that in the stratum oriens, stratum radiatum, and stratum moleculare of CA1, Kv1.1, Kv1.2, and Kv1.4 are located presynaptically on afferent inputs. As described above and previously (Rhodes et al., 1997), it remains a possibility that a small proportion of the immunoreactivity for Kv1.1, Kv1.2, and Kv1.4 is located postsynaptically on the cell bodies and dendrites of CA1 pyramidal cells and interneurons.

## Kainic acid lesions of the CA3 subfield

Given the very high levels of Kv1.1 mRNA expression in CA3 pyramidal cells, and because CA3 and CA1 ibotenic acid lesions



*Figure 7.* Effects of a large kainic acid lesion in the CA3 subfield on Kv1 $\alpha$ and $\beta$ subunit immunoreactivity in CA3 and CA1. As shown in the sections stained for Nissl substance (*A, B*), this kainic acid lesion killed neurons along the entire mediolateral and dorsoventral extent of CA3 but spared neurons within the CA1 subfield. The major effect of this lesion was to dramatically reduce the density of Kv1.1 immunoreactivity within the stratum radiatum of CA3 and CA1 (compare *C, D, asterisks*). Interestingly, this lesion also appeared to reduce slightly the density of Kv1.4 and Kv1.2 immunoreactivity in the stratum radiatum of CA3 and CA1. Together, these results suggest that in the stratum radiatum of CA1, Kv1.1, Kv1.4, and Kv1.2 are all associated with the axons and terminals of the Schaffer collateral pathway. Consistent with the results presented in Figures 5 and 6, this large CA3 lesion did not appear to reduce the density of Kv1.1 (*D*) or Kv1.4 (*F*) immunoreactivity in the stratum lucidum of CA3 (*arrowheads*). Because this lesion destroyed CA3 pyramidal cells, this result also confirms that Kv1.1 and Kv1.4 immunoreactivity in CA3 is associated with mossy fiber axons.

failed to alter the density of Kv1.1 immunoreactivity in CA1, we decided to produce a more complete lesion of CA3. To accomplish this, we took advantage of the observation that CA3 pyramidal cells are highly sensitive to the neurotoxin kainic acid (Bernard and Wheal, 1995). Unilateral CA3 lesions using kainic acid, injected into the lateral cerebral ventricle immediately adjacent to the CA3 subfield, were made in six animals. An example of the effects of such a lesion is shown in Figure 7. This lesion destroyed the entire CA3 subfield, as evidenced by the loss neurons in Nissl-stained sections and by the necrotic tissue in the stratum radiatum of CA3 (Fig. 7*B*). This lesion also destroyed the large polymorphic neurons in the hilus of the dentate gyrus as well as a subpopulation of pyramidal cells in the subiculum. Importantly, pyramidal cells in CA1 appeared to be spared by this

lesion, and there did not appear to be any neuronal loss in the contralateral hippocampus.

Unlike the circumscribed ibotenic acid lesion (Fig. 5), the complete CA3 kainic acid lesion eliminated the vast majority of Kv1.1 immunoreactivity in the stratum radiatum of CA1, suggesting that Kv1.1 is located on the axons and terminals of the Schaffer collateral pathway (Fig. 7, compare *C, D*). Some Kv1.1 immunoreactivity remained after these large CA3 lesions; this weak Kv1.1 staining appeared to be diffusely distributed in the dendrites of hippocampal pyramidal cells. Surprisingly, the density of Kv1.2 and Kv1.4 immunoreactivity in the stratum radiatum of CA3 and CA1 was also reduced after this lesion (Fig. 7*E–H*), suggesting that these two subunits may also be located on axons and terminals of the Schaffer collateral pathway. Together, these results suggest that in the stratum radiatum of CA1, a large proportion of Kv1.1 immunoreactivity is located on the axons and terminals of the Schaffer collateral pathway and that these terminals also contain, albeit at a far lower density, Kv1.2 and Kv1.4.

## Effects of fornix transections on Kv1 $\alpha$ and $\beta$ subunit immunoreactivity

As described previously (Rhodes et al., 1996), Kv$\beta$2 mRNA is expressed in large neurons in the medial septal and diagonal band nuclei. This pattern corresponds well to the patterns of Kv1.1, Kv1.2, and Kv1.4 expression in these structures (K. J. Rhodes, M. M. Monaghan, N. X. Barrezueta, and J. S. Trimmer, unpublished observations), suggesting that all four of these subunits are expressed in neurons known to provide subcortical cholinergic input to the hippocampal formation (Mesulam et al., 1983). To explore the association of Kv1 family $\alpha$ and $\beta$ subunits with septal and other subcortical afferents to the hippocampus, seven animals sustained a unilateral transection of the fornix. Although the fornix transections completely eliminated histochemical staining for AChE within the ipsilateral dentate gyrus and CA subfields, these lesions did not have any detectable effect on the distribution or density Kv1.1, Kv1.2, Kv1.4, or Kv$\beta$2 immunoreactivity within the hippocampal formation (results not shown). This result indicates that these subunits are not located presynaptically on cholinergic afferents or on other subcortical inputs that reach the hippocampus via the fornix.

## Association of Kv $\alpha$ and $\beta$ subunits in hippocampal K$^+$ channel complexes

The pattern of immunoreactivity for Kv1.1, Kv1.2, Kv1.4, and Kv$\beta$2 in hippocampal formation and the results of our lesion analyses predict that these subunits are associated with one another in heteromultimeric K$^+$ channel complexes located on excitatory projections. To determine the extent of association of Kv1.1, Kv1.2, Kv1.4, and Kv$\beta$2 in rat hippocampal K$^+$ channel complexes, we performed reciprocal coimmunoprecipitation experiments using subunit-specific antibodies. Detergent lysates were prepared from rat hippocampal membranes under conditions previously shown to preserve $\alpha$–$\beta$ subunit interactions (Rhodes et al., 1995, 1996, 1997; Nakahira et al., 1996; Shi et al., 1996). For each subunit, immunoprecipitation reactions were performed under conditions of antibody excess, which was verified by subsequent removal and analysis of the depleted supernatant after pelleting the immunoprecipitation reaction product. In each case all recoverable antigen was removed by the initial immunoprecipitation reaction. Immunoprecipitation products, representing immunopurified channel complexes, were then subjected to immunoblot analyses to assay for the presence of the specific $\alpha$ and $\beta$ subunit polypeptides (Fig. 8).
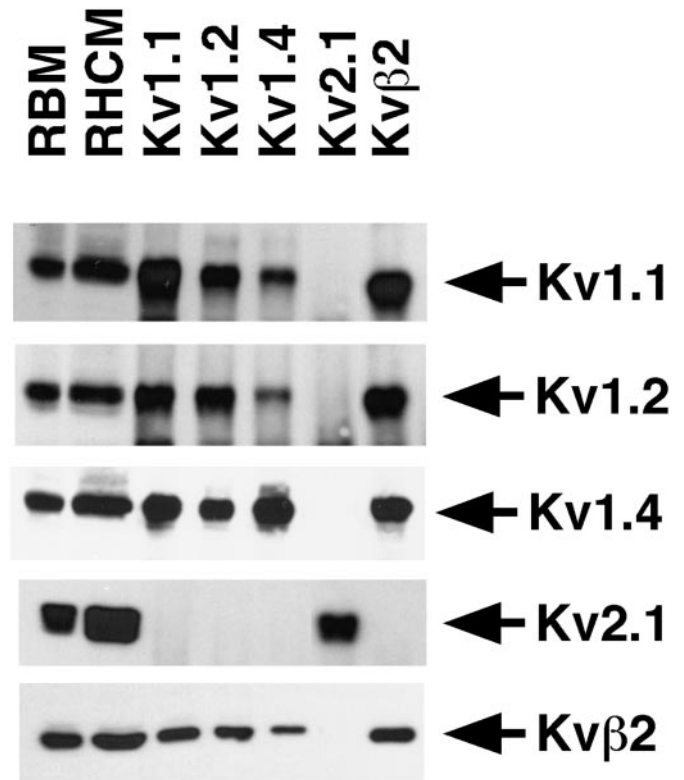


*Figure 8.* Heteromeric Kv1 $\alpha$ and $\beta$ subunit channel complexes in the rat hippocampus. Detergent lysates of adult rat brain membranes (*RBM*, 30 $\mu$g) and rat hippocampal membranes (*RHCM*, 20 $\mu$g), and aliquots of products of immunoprecipitation reactions performed on detergent extracts of 83 $\mu$g of RHCM with the indicated rabbit polyclonal antibodies were size-fractionated by 9% ($\alpha$ subunit blots) or 12% (Kv$\beta$2 blot) SDS-PAGE. Samples were transferred to nitrocellulose and probed with affinity-purified rabbit anti-Kv1 $\alpha$ subunit-specific polyclonal antibodies or mouse anti-Kv$\beta$2 mAb K17/70. Bound antibody was detected by ECL and autoradiography. *Arrows* point to the band resulting from specific detection of the antigen listed to the *right*. For clarity, only the section of the immunoblot containing the cognate antigen is shown.

Reciprocal immunoblots were performed using antibodies specific for each of the $\alpha$ and $\beta$ subunit polypeptides. Each of the affinity-purified rabbit polyclonal anti-$\alpha$ subunit antibodies could directly immunoprecipitate the respective $\alpha$ subunit from the brain membrane extracts (Fig. 8). Overall, clear evidence for association of Kv1.1, Kv1.2, Kv1.4, and Kv$\beta$2 in hippocampal K$^+$ channel complexes was obtained. Although quantitative analyses were not performed, comparison of the relative intensities of bands visible on our immunoblots, which were performed under conditions of antibody excess, indicted that most of the Kv1.1, Kv1.2, and Kv1.4 pools in the hippocampus are associated with the cytoplasmic Kv$\beta$2 subunit. The pool of Kv1.1 seemed split between that associated with Kv1.2 and Kv1.4, whereas Kv1.2 was predominantly associated with Kv1.1 and to a lesser extent with Kv1.4. Consistent with this, complexes immunopurified with anti-Kv1.1 antibodies contained the greater part of hippocampal Kv1.4, with less of the Kv1.4 present in complexes containing Kv1.2. Kv2.1, which has a somatodendritic localization on both principal cells and interneurons in the hippocampus (Rhodes et al., 1995, 1997), could not be detected in hippocampal K$^+$ channel complexes containing Kv1.1, Kv1.2, Kv1.4, or Kv$\beta$2. Overall, these results suggest that Kv1.1, Kv1.2, and Kv1.4 associate with one another in hippocampal K$^+$

## Dentate Gyrus
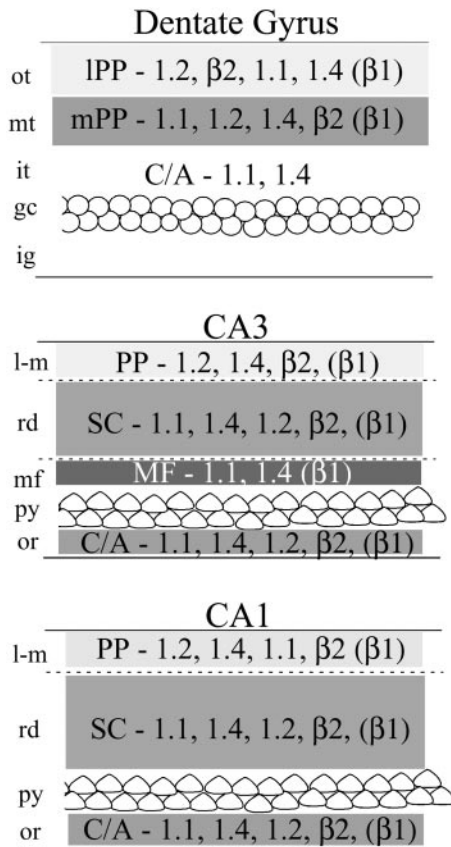


*Figure 9.* Summary of the localization of Kv1.1, Kv1.2, Kv1.4, and Kvβ2 across hippocampal subfields. This summary figure is derived from the results of our analysis of systematic lesions and the effects of these lesions on the staining patterns for the indicated subunit. In each lamina, the subunits are ordered according to their relative staining intensity, from high to low. Although the distribution of Kvβ1 was not examined in the present study, we have reported the distribution of Kvβ1 previously (Rhodes et al., 1997) and included our interpretation of its localization in this summary figure. *C/A*, Commissural/associational pathway; *lPP*, lateral perforant path; *mPP*, medial perforant path; *PP*, perforant path; *SC*, Schaffer collaterals; *MF*, mossy fiber zone; *ot*, outer-third of the molecular layer; *mt*, middle third of the molecular layer; *it*, inner third of the molecular layer; *gc*, granule cell layer; *ig*, infragranular layer; *l-m*, stratum lacunosum moleculare; *rd*, stratum radiatum; *py*, stratum pyramidale; *or*, stratum oriens.

channel complexes and that many of these complexes contain at least one Kvβ2 subunit.

## DISCUSSION

In summary, the results described above indicate that Kv1 channels containing the Kv1.1, Kv1.2, Kv1.4, and Kvβ2 subunits are associated with the axons and terminal fields of the major cortical afferent input and the major intrinsic projections within the rat hippocampal formation (Fig. 9). Although the mRNA for each subunit is expressed in the cells of origin of these projections, the comparative lack of immunoreactivity in the somata of principal cells indicates that these subunits are efficiently transported out of the cell body and targeted to axonal and nerve terminal domains. This relationship between mRNA expression and protein localization is similar to that reported for the cerebellum (McNamara et al., 1993, 1996; Rhodes et al., 1996, 1997) and spinal cord (Rasband and Trimmer, 2001). Ibotenic or kainic acid lesions altered the density of Kv1 α and β subunit immunoreactivity in

the termination fields of cells destroyed by the lesion. Lesions placed within those termination fields, however, were generally without effect on the distribution of immunoreactivity within the boundaries of the lesion. Two clear exceptions to this general pattern are the loss of Kvβ2 immunoreactivity in the apical dendrites of CA1–CA3 pyramidal cells caused by lesions within these subfields and the increased density of Kv1.1 immunoreactivity within the boundaries of ibotenic acid lesions in CA3 or CA1. The reason for the selective increase in Kv1.1 immunoreactivity within the boundaries of these two lesions is unclear but is unlikely to represent a staining artifact, because it did not occur with the other rabbit polyclonal antibodies or in control sections in which the primary antibody was omitted. Therefore, the increase in Kv1.1 density may represent an attempt by these circuits to alter the subunit composition of Kv1 channels in response to perturbations of the Schaffer collateral pathway. Nonetheless, the use of complementary lesions allows us to distinguish between changes in immunoreactivity resulting from axonal degeneration and changes in immunoreactivity caused by altered morphology in the postsynaptic target. This is a powerful approach for associating immunohistochemical staining patterns with specific anatomical pathways (Rouse and Levey, 1997).

Although the results from the present study are consistent with previous interpretations of Kv1 α and β subunit staining patterns in the hippocampus (Wang et al., 1993; Rhodes et al., 1995, 1996, 1997; Cooper et al., 1998), they are at odds with the conclusions of Veh et al. (1995) and Sheng et al. (1994). In particular, Veh et al. (1995) concluded that the majority of Kv1.1 immunoreactivity in the dentate gyrus and CA subfields is associated with the dendrites of granule and pyramidal cells, respectively, and Sheng et al. (1994) reported intense Kv1.2 immunoreactivity throughout the apical dendritic arbors of hippocampal pyramidal cells and in mossy fiber terminals in CA3. Although the reasons for the differences in the data are unclear, one reasonable explanation is that Veh et al. (1995) interpreted their staining as dendritic when in fact it was concentrated in axons and terminals. As mentioned above, interpretation of staining patterns in the absence of direct experimental support can be difficult, particularly in regions such as CA3 and CA1, where there is both a dense ramification of dendritic arbors and dense synaptic innervation. A second reasonable explanation of the differences between these data are that the antibodies and immunohistochemical procedures (e.g., fixation and tissue sectioning) were different. Regardless of which explanation is correct, our results, which demonstrate a clear relationship among mRNA expression patterns, immunohistochemical staining, coimmunoprecipitation, and the results of systematic and complementary lesions, suggest that the majority of Kv1 α subunit immunoreactivity is associated with axons and terminals of excitatory pathways and not with somata and dendrites of hippocampal neurons.

Although the complementary lesion analysis described above can account for and explain the origin of most Kv1 α and β subunit immunoreactivity in the hippocampus, one area of uncertainty is the inner third of the molecular layer of the dentate gyrus. We observed that the density of Kv1.1 and Kv1.4 immunoreactivity increases after ibotenic acid lesions of the entorhinal cortex and remains unchanged after circumscribed ibotenic acid lesions in the dentate gyrus. The most parsimonious explanation for these results is that in the inner third, Kv1.1 and Kv1.4 are associated with subcortical afferents to the dentate gyrus or with axons of the commissural/associational (C/A) pathway. The latter pathway is formed by the mossy cells and other interneuron in

the dentate hilus (Laatsch and Cowan, 1967; Amaral and Witter, 1989). The lack of an effect of fornix lesions on Kv1.1 and Kv1.4 immunoreactivity makes it unlikely that subcortical afferents are the source of the staining in the inner third. Although we did not attempt to disrupt the C/A pathway directly, there is some evidence from our data to indicate that Kv1.1, Kv1.4, and Kv1.2 are associated with axons and terminals of this projection. As described in Results, our kainic acid lesions of the CA3 subfield also destroyed neurons in the hilus of the dentate gyrus that give rise to the C/A pathway. Careful examination of these cases (Fig. 7) indicates that in the ipsilateral dentate gyrus there is a reduction in the density of Kv1.1, Kv1.2, and Kv1.4 immunoreactivity in the inner third of the molecular layer, suggesting that these subunits are located on the terminals of the dentate C/A pathway. This observation should be followed up with direct surgical lesions (Rouse and Levey, 1997).

Together with the immunohistochemical staining, the results of our coimmunoprecipitation analyses indicate that there is a complex and heterogeneous association of Kv1 $\alpha$ subunits across hippocampal subfields. Interestingly, our data indicated that the total pool of Kv1.1 is split between complexes containing Kv1.4 or Kv1.2 and that the majority of Kv1.4-containing complexes also contained Kv1.1, with less Kv1.4 coassociated with Kv1.2. These results correspond well with the immunohistochemical findings, in that Kv1.4 is colocalized with Kv1.1 in the perforant path, mossy fiber pathway, and Schaffer collaterals, and Kv1.2 is colocalized with Kv1.1 in the perforant path and Schaffer collaterals. In areas such as the dentate gyrus, Kv1.4 and Kv1.2 may be coassociated on some, but not all, perforant path terminals, although it appears that these two subunits are colocalized. In the middle third of the dentate molecular layer, for example, it is clear that the staining for Kv1.2 and Kv1.4 overlaps, but entorhinal lesions have distinct effects on their distribution, indicating that these two subunits may be associated with separate or only partly overlapping sets of entorhinal afferents. Although the coimmunoprecipitation results indicate that most of the Kv1 $\alpha$ subunit pool in the hippocampus is coassociated with the Kv$\beta$2 $\beta$ subunit, the immunohistochemical data clearly indicate that some Kv$\beta$2 immunoreactivity is concentrated in domains that do not have a corresponding high density of Kv1.1, Kv1.2, or Kv1.4. Although the strong staining for Kv$\beta$2 in the apical dendrites of CA pyramidal cells indicates that there is likely to be a Kv1 family $\alpha$ subunit located postsynaptically in hippocampal pyramidal cells, it is not clear which Kv1 subunit this may be. Alternative explanations for the "excess" Kv$\beta$2 are that in these locations Kv$\beta$2 interacts with $\alpha$ subunits from other Kv channel families (Yang et al., 2001), or that it functions autonomously, perhaps as an oxidoreductase enzyme (McCormack and McCormack, 1994; Gulbis et al., 1999). Thus it is possible that in pyramidal cell dendrites, Kv$\beta$2 serves functions unrelated to its role as an integral component of Kv1 channels.

Although the data reported here are consistent with the demonstration that DTX-sensitive Kv channels modulate neurotransmitter release by direct action at nerve terminals (Dorandeau et al., 1997; Schechter, 1997; Southan and Owen, 1997; Geiger and Jonas, 2000), they do not indicate that Kv1.1 and Kv1.2 contribute to the DTX-sensitive transient K⁺ conductance that has been observed in the dendrites of rat and mouse hippocampal pyramidal cells (Halliwell et al., 1986; Storm 1990; Wu and Barish, 1992; Golding et al., 1999). There are several likely explanations for this discrepancy. One is that there may be other DTX-sensitive $\alpha$ subunits not studied in this report, such as Kv1.6, located on the

dendrites of hippocampal pyramidal cells. A second explanation is that the minor component of the Kv1.1 or Kv1.2 immunoreactivity that remains after our lesions is located on the dendrites of hippocampal pyramidal cells in sufficient density to form measurable DTX-sensitive currents.

The coimmunoprecipitation and immunohistochemical data described here and in previously published work suggest that the biophysical properties of Kv1 $\alpha$ and $\beta$ subunits vary across hippocampal pathways. In the mossy fiber pathway, the colocalization and likely coassociation of Kv1.1 and Kv1.4, in a complex that also contains Kv$\beta$1 (Rhodes et al., 1997), would be expected to give rise to a rapidly inactivating DTX-sensitive K⁺ conductance located on mossy fiber axons and terminals. In fact, a DTX-sensitive A-type current has been directly observed in patch-clamp analyses of mossy-fiber terminals in rat hippocampal slices (Geiger and Jonas, 2000). A DTX-sensitive A-type current having a similar subunit composition would be expected on some perforant path terminals in the dentate gyrus, whereas a separate population of perforant path terminals may contain a Kv1.2 in association with Kv$\beta$ 2, forming a slowly inactivating DTX-sensitive K⁺ current. In the CA1 subfield, the coassociation and colocalization of Kv1.1, Kv1.2, and Kv1.4, together with Kv$\beta$1 (Rhodes et al., 1997), would be expected to form another DTX-sensitive A-type current modulating glutamate release from terminals of the Schaffer collateral pathway. Clearly, the heteromultimerization of Kv1 subunits provides a molecular substrate for presynaptic modulation of glutamate release in a pathway-specific manner. Moreover, the biophysical properties of channels containing these subunits can be altered by phosphorylation (Levitan, 1999), providing a potent mechanism for dynamic regulation of neurotransmitter release.

The importance of DTX-sensitive Kv1-family K⁺ channels to hippocampal function has long been recognized. The pioneering studies of Halliwell and Dolly (1982) and Halliwell et al. (1986) showed that the epileptogenic effects of DTX were attributable to increased neurotransmitter release, and that this toxin binds to components present at terminal regions to mediate its preferential effect in the hippocampus. These studies also identified a transient K⁺ conductance as a major target for the effects of DTX in CA1 pyramidal cells (Halliwell et al., 1986). Subsequent studies revealed an important role for DTX-sensitive transient or A-type conductance in the hippocampus (Storm, 1990). The importance of axonal A-type currents in hippocampal mossy fiber terminals has also been shown in more recent studies, which have implicated rapidly inactivating, DTX-sensitive axonal Kv channels as the main molecular determinants of activity-dependent spike broadening (Geiger and Jonas, 2000). Such dynamic modification of action potential shape impacts both Ca²⁺ influx and glutamate release at mossy fiber terminals and as such would be expected to augment synaptic transmission at mossy fiber synapses. Our results showing the association of Kv1.1 and Kv1.4 in hippocampal membranes, and the colocalization of these and other Kv1-family $\alpha$ subunits in hippocampal circuits, point toward a significant contribution of heteromeric Kv1 channels to activity-dependent spike broadening and regulation of excitatory transmitter release within mammalian hippocampal formation.

## REFERENCES

Acsády L, Kamondi A, Sík A, Freund T, Buzáki G (1998) GABAergic cells are the major postsynaptic targets of mossy fibers in the rat hippocampus. J Neurosci 18:3386–3403.
Amaral DG, Witter MP (1989) The three dimensional organization of

the hippocampal formation: a review of anatomical data. Neurosci 31:571–591.

Bernard C, Wheal HV (1995) Plasticity of AMPA and NMDA receptor-mediated epileptiform activity in a chronic model of temporal lobe epilepsy. Epilepsy Res 21:95–107.

Chandy KG, Gutman GA (1995) Voltage-gated potassium channel genes. In: Ligand and voltage-gated ion channels (North RA, ed), pp 1–71. Boca Raton, FL: CRC.

Cooper EC, Milroy A, Jan YN, Jan LY, Lowenstein DH (1998) Presynaptic localization of Kv1.4-containing A-type potassium channels near excitatory synapses in the hippocampus. J Neurosci 18:965–974.

Dolorfo CL, Amaral DG (1998) Entorhinal cortex of the rat: topographic organization of the cells of origin of the perforant path projection to the dentate gyrus. J Comp Neurol 398:25–48.

Dorandeu F, Wetherell J, Pernot-Marino I, Tattersall JEH, Fosbraey P (1997) Effects of excitatory amino acid antagonists on dendrotoxin-induced increases in neurotransmitter release and epileptiform bursting in rat hippocampus in vitro. J Neurosci Res 48:499–506.

Erselius RT, Wree A (1991) Ultrastructure of axons in stereotaxically placed ibotenic acid-induced lesions of the hippocampus in the adult rat. Evidence for demyelination and degeneration of dispersed axons of passage. J Hirnforschung 32:139–148.

Geiger JRP, Jonas P (2000) Dynamic control of presynaptic Ca$^{2+}$ inflow by fast-inactivating K$^+$ channels in hippocampal mossy fiber boutons. Neuron 28:927–939.

Golding NL, Jung H, Mickus T, Spruston N (1999) Dendritic calcium spike initiation and repolarization are controlled by distinct potassium channel subtypes in CA1 pyramidal neurons. J Neurosci 19:8789–8798.

Gulbis JM, Mann S, MacKinnon R (1999) Structure of a voltage-dependent K$^+$ channel beta subunit. Cell 97:943–952.

Halliwell JV, Dolly JO (1982) Preferential action of beta-bungarotoxin at nerve terminal regions in the hippocampus. Neurosci Lett 30:321–327.

Halliwell JV, Othman IB, Pelchen-Matthews A, Dolly JO (1986) Central action of dendrotoxin: selective reduction of a transient K$^+$ conductance in hippocampus and binding to localized acceptors. Proc Natl Acad Sci USA 83:493–497.

Hoffman DA, Magee JC, Colbert CM, Johnston D (1997) K+ channel regulation of signal propagation in dendrites of hippocampal pyramidal neurons. Nature 387:869–875.

Hu PS, Benishin C, Fredholm CC (1991) Comparison of the effects of four dendrotoxin peptides, 4-aminopyridine and tetraethylammoinium on the electrically evoked ($^3$H)noradrenaline release form rat hippocampus. Eur J Pharmacol 209:87–93.

Ishizuka N, Weber J, Amaral DG (1990) Organization of intrahippocampal projections originating from CA3 pyramidal cells in the rat. J Comp Neurol 295:580–523.

Johnson DAG, Sportsman JR, Elder JH (1984) Improved techniques utilizing nonfat dry milk for analysis of proteins and nucleic acids transferred to nitrocellulose. Gene Anal Tech 1:3–8.

Johnston D, Hoffman DA, Magee JC, Poolos NP, Watanabe S, Colbert CM, Migliore M (2000) Dendritic potassium channels in hippocampal pyramidal neurons. J Physiol (Lond) 525:75–81.

Kohler C, Schwarcz R (1983) Comparison of ibotenate and kainate neurotoxicity in rat brain: a histological study. Neurosci 8:819–835.

Laatsch R, Cowan WM (1967) Electron microscopic studies of the dentate gyrus of the rat II. Degeneration of commissural afferents. J Comp Neurol 130:241–262.

Levitan IB (1999) Modulation of ion channels by protein phosphorylation. How the brain works. Adv Second Messenger Phosphoprotein Res 33:3–22.

McCormack T, McCormack K (1994) *Shaker* K$^+$ channel beta subunits belong to an NAD(P)H-dependent oxidoreductase superfamily. Cell 79:1133–1135.

McNamara NM, Muniz ZM, Wilkin GP, Dolly JO (1993) Prominent location of a K$^+$ channel containing the alpha subunit Kv1.2 in the basket cell nerve terminals of rat cerebellum. Neuroscience 57:1039–1045.

McNamara NM, Averill S, Wilkin GP, Dolly JO, Priestley JV (1996) Ultrastructural localization of a voltage-gated K$^+$ channel alpha subunit (Kv1.2) in the rat cerebellum. Eur J Neurosci 8:688–699.

Mesulam MM, Mufson EJ, Wainer BH, Levey AI (1983) Central cholinergic pathways in the rat: an overview based on an alternative nomenclature (Ch1-Ch6). Neuroscience 10:1185–1201.

Nakahira K, Shi G, Rhodes KJ, Trimmer JS (1996) Selective interaction of voltage-gated K$^+$ channel beta subunits with alpha subunits. J Biol Chem 271:7084–7089.

Rasband MN, Trimmer JS (2001) Subunit composition and novel localization of K$^+$ channels in spinal cord. J Comp Neurol 429:166–176.

Rhodes KJ, Keilbaugh SA, Barrezueta NX, Lopez KL, Trimmer JS (1995) Association and colocalization of K$^+$ channel $\alpha$- and $\beta$-subunit polypeptides in rat brain. J Neurosci 15:5360–5371.

Rhodes KJ, Monaghan MM, Barrezueta NX, Nawoschik S, Bekele-Arcuri Z, Matos M, Nakahira K, Schechter LE, Trimmer JS (1996) Voltage-gated K$^+$ channel $\beta$ subunits: expression and distribution of Kv$\beta$1 and Kv$\beta$2 in adult rat brain. J Neurosci 16:4846–4860.

Rhodes KJ, Strassle BW, Monaghan MM, Bekele-Arcuri Z, Matos MF, Trimmer JS (1997) Association and colocalization of Kv$\beta$1 and Kv$\beta$2 with Kv1 $\alpha$-subunits in mammalian brain K$^+$ channel complexes. J Neurosci 17:8246–8258.

Rouse ST, Levey AI (1997) Muscarinic acetylcholine receptor immunoreactivity after hippocampal commissural/associational pathway lesions: evidence for multiple presynaptic receptor subtypes. J Comp Neurol 380:382–394.

Schechter LE (1997) The potassium channel blockers 4-aminopyridine and tetraethylammonium increase the spontaneous basal release of [$^3$H]5-hydroxytryptamine in rat hippocampal slices. J Pharmacol Exp Ther 282:262–270.

Scott VE, Muniz Z, Sewing S, Lichtinghagen R, Parcej DN, Pongs O, Dolly JO (1994) Antibodies specific for distinct Kv subunits unveil a heterooligomeric basis for subtypes of alpha-dendrotoxin-sensitive K$^+$ channels in bovine brain. Biochemistry 33:1617–1623.

Séquier JM, Brennand J, Barhanin J, Lazdunski M (1990) Regional expression of a MCD-peptide and dendrotoxin I-sensitive voltage-dependent potassium channel in rat brain. FEBS Lett 263:163–165.

Sheng M, Liao YJ, Jan YN, Jan LY (1993) Presynaptic A-current based on heteromultimeric K$^+$ channels detected in vivo. Nature 365:72–75.

Sheng M, Tsaur ML, Jan YN, Jan LY (1994) Contrasting subcellular localization of the Kv1.2 K$^+$ channel subunit in different neurons of rat brain. J Neurosci 14:2408–2417.

Shi G, Kleinklaus AK, Marrion NV, Trimmer JS (1994) Properties of Kv2.1 K$^+$ channels expressed in transfected mammalian cells. J Biol Chem 269:23204–23211.

Shi G, Nakahira K, Hammond S, Rhodes KJ, Schechter LE, Trimmer JS (1996) Beta subunits promote K$^+$ channel surface expression through effects early in biosynthesis. Neuron 16:843–852.

Southan AP, Owen DG (1997) The contrasting effects of dendrotoxins and other potassium channel blockers in the CA1 and dentate gyrus regions of rat hippocampal slices. Br J Pharmacol 122:335–343.

Steward O (1976) Topographic organization of the projections from the entorhinal area to the hippocampal formation of the rat. J Comp Neurol 167:285–314.

Steward O, Scoville SA (1976) Cells of origin of the entorhinal cortical afferents to the hippocampus and fascia dentata of the rat. J Comp Neurol 169:347–370.

Storm JF (1990) Potassium currents in hippocampal pyramidal cells. Prog Brain Res 83:161–187.

Swanson LW, Wyss JM, Cowan WM (1978) An autoradiographic study of the organization of intrahippocampal association pathways in the rat. J Comp Neurol 181:681–716.

Tago H, Kimura H, Maeda T (1986) Visualization of detailed acetylcholinesterase fiber and neuron staining in rat brain by a sensitive histochemical procedure. J Histochem Cytochem 34:1431–1438.

Tamamaki N, Nojyo Y (1988) Three-dimensional analysis of the whole axonal arbors originating from single CA2 pyramidal neurons in the rat hippocampus with the aid of a computer graphic technique. Brain Res 452:255–272.

Trimmer JS (1991) Immunological identification and characterization of a delayed rectifier K+ channel polypeptide in rat brain. Proc Natl Acad Sci USA 88:10764–10768.

Veh RW, Lichtinghagen R, Sewing S, Wunden F, Grumbach IM, Pongs O (1995) Immunohistochemical localization of five members of the Kv1 channel subunits: contrasting subcellular locations and neuron-specific colocalizations in rat brain. Eur J Neurosci 7:2189–2205.

Wang H, Kunkel DD, Martin TM, Schwartzkroin PA, Tempel BL (1993) Heteromultimeric K$^+$ channels in terminal and juxtaparanodal regions of neurons. Nature 365:75–79.

Wang H, Kunkel DD, Schwartzkroin PA, Tempel BL (1994) Localization of Kv1.1 and Kv1.2, two K$^+$ channel proteins, to synaptic terminals, somata, and dendrites in the mouse brain. J Neurosci 14:4588–4599.

Witter MP, Griffionen AW, Jorritsma BB, Krijnen JL (1988) Entorhinal projections to the hippocampal CA1 area in the rat: an underestimated pathway. Neurosci Lett 85:193–198.

Wu RL, Barish ME (1992) Two pharmacologically and kinetically distinct transient potassium currents in cultured embryonic mouse hippocampal neurons. J Neurosci 12:2235–2246.

Wyss JM (1981) An autoradiographic study of the efferent connections of the entorhinal cortex in the rat. J Comp Neurol 199:495–512.

Yang E-K, Alvira MR, Levitan ES, Takimoto K (2001) Kv subunits increase expression of Kv4.3 channels by interacting with their C termini J Biol Chem 276:4839–4844.

Zhang L, McBain CJ (1995) Potassium conductances underlying repolarization and after-hyperpolarization in rat CA1 hippocampal interneurones. J Physiol (Lond) 488:661–672.